
NJC
New Journal of Chemistry
A journal for new directions in chemistry

Cite this: DOI: 10.1039/c0xx00000x

www.rsc.org/xxxxxx

PAPER

Amorphous NiO Electrocatalyst Overcoated ZnO Nanorod Photoanode for Enhanced Photoelectrochemical Performance

Yanchao Mao,[a] Yongguang Cheng,[a] Junqiao Wang,[a] Hao Yang,[b] Mingyang Li,[b] Jian Chen,[c] Mingju Chao,[a] Yexiang Tong,[b] Erjun Liang[a*]

Received (in XXX, XXX) Xth XXXXXXXXX 20XX, Accepted Xth XXXXXXXXX 20XX
DOI: 10.1039/b000000x

Developing high-performance photoanodes is essential for practical applications of photoelectrochemical (PEC) water splitting. In this work, we demonstrated that introducing amorphous NiO electrocatalysts to the surface of ZnO nanorod (NR) photoanodes can largely improve their PEC performance. The NiO/ZnO core-shell NR arrays were obtained by two step electrodepositions and annealing. The amorphous NiO nanosheet electrocatalyst shell on single crystalline ZnO NR semiconductor core formed a composite photoanode configuration for PEC water splitting. The NiO/ZnO photoanode yielded a remarkable 260 mV cathodic shift in the onset potential for water oxidation compared to the bare ZnO photoanode. And the highest PEC efficiency of the NiO/ZnO photoanode was found to be 1.81%, which is 30 times higher than that of the ZnO photoanode (0.06%). This research demonstrates that introducing amorphous NiO electrocatalysts can largely improve the PEC performance of ZnO photoanodes.

Introduction

As an effective solar energy conversion technique, photoelectrochemical (PEC) water splitting has attracted great attention because it offers the capability of harvesting solar energy to generate hydrogen.[1] A series of metal oxides e.g. α-Fe_2O_3,[2] TiO_2,[3] and ZnO[4] have been applied as photoanodes for PEC water splitting. Nevertheless, there are still numerous challenges in the development of high-performance photoanodes. A complete PEC water splitting process includes light absorption, generating electron-hole pairs, charge transport, and catalysis for water redox reactions. Therefore, an ideal photoanode should possess appropriate band structure, good light harvesting ability, low recombination rate of electron-hole pairs, good conductivity, and high catalytic activity for water redox reactions. So far, there is not a single material having all these merits of the an ideal photoanode. For instance, α-Fe_2O_3 is a promising photoanode material due to its appropriate band structure for ultilizing visible light and high theoretical solar-to-hydrogen conversion efficiency of 15%.[5] However, the reported conversion efficiencies of α-Fe_2O_3 photoanodes are considerably lower than the theoretical value owing to several limiting factors such as low absorption coefficient, insulator-like conductivity, and poor oxygen evolution reaction kinetics.[6] TiO_2 has also been extensively studied as an PEC photoanode because it has excellent stability and good catalytic property, and its appropriate valence and conduction band edges beyond the oxidation and reduction potential of water respectively.[7] Nevertheless, its low conductivity and wide bandgap that can not harvest visible light remain as obstacles for achieving a high conversion efficiency. ZnO has a similar band structure with TiO_2,[8] and the typical electron mobility of ZnO is 10-100 times higher than that of TiO_2,[9] which make ZnO a very promising candidate for PEC water splitting. However, owing to the high recombination rate of electron–hole pairs and poor catalytic activity for water oxidation reaction,[10] the reported PEC efficiency of ZnO photoanode is still much lower than TiO_2.

Recently, considerable research efforts have been devoted to introducing electrocatalysts to the surface of photoanode, which could promote surface oxygen evolution reaction of photoanodes. For example, Co-Pi electrocatalysts have been used to improve the PEC performance of α-Fe_2O_3,[11] WO_3,[12] and $BiVO_4$.[13] Meanwhile, a series of Ni-based electrocatalysts e.g. nickel borates,[14] nickel hydroxides,[15] nickel oxides,[16, 17] and nickel cobaltite[18] exhibited excellent catalytic performance for water oxidation reaction. Nickel hydroxide[19] and nickel oxide[20] electrocatalysts have been also shown to improve the PEC performance of photoanodes. In addition, superior electrocatalytic activity in water oxidation reaction was demonstrated from amorphous electrocatalytic materials compared to their crystalline phase, including Fe_2O_3,[21] CoO_x,[21] and RuO_2[22]. It is because these amorphous electrocatalysts have larger density of active surface unsaturated sites and higher degree of atomic structural flexibility than their crystalline phase.[21, 22] Up to now, many composite photoanodes e.g. $ZnFe_2O_4$/ZnO,[23, 24] CdTe/ZnO,[25, 26] CdSe/ZnO,[27] CdSe/CdS/ZnO,[28] Pt/ZnO,[29] g-C_3N_4/ZnO,[30] g-C_3N_4/Pt/ZnO,[31] BiOI/ZnO,[32, 33] $Ni(OH)_2$/ZnO,[19] CoNi double hydroxide/ZnO,[34] etc. have been developed to improve the PEC performance of ZnO. In this work, we introduced amorphous NiO electrocatalysts onto the surface of conventional ZnO photoanode to overcome its limitations and improve the PEC performance. The amorphous NiO/single crystalline ZnO core-shell nanorod (NR) arrays photoanode exhibited a remarkable cathodic shift in onset potential for water oxidation and a significant enhancement of PEC efficiency compared to the bare ZnO photoanode. This research demonstrated that introducing amorphous NiO electrocatalysts can advantageously impact the PEC performance of conventional ZnO photoanode.

Experimental section

Fabrication of NiO/ZnO Core-shell NR Arrays

All reagents in this study were of analytical grade. Electrodeposition experiments were performed in a conventional three-electrode cell. A graphite rod and a saturated calomel electrode (SCE) was used as the counter electrode and reference electrode, respectively. The working electrode was the F-doped SnO_2 coated glass (FTO) glass with a sheet resistance of 14 Ω/sq. The FTO glass was ultrasonically cleaned in deionized (DI) water, then ethanol, and it was finally washed by DI water again before electrodeposition. The ZnO NR arrays were synthesized through cathodic electrdeposition in a solution containing 0.02 M $Zn(NO_3)_2$ + 0.01 M CH_3COONH_4 + 0.01 M $(CH_2)_6N_4$ under a current density of 0.5 mA cm^{-2} for 1 h at 90 °C. The secondary electrodeposition was carried out on the as-synthesized ZnO NR arrays in a solution of 0.01 M $NiCl_2$ + 0.02 M NH_4NO_3 at 1 mA cm^{-2} for 3 min at 70 °C. After the two-step electrodeposition, the sample was rinsed in DI water, and then was dried in air at room temperature before annealing. The as-deposited samples were further annealed in air at 300 °C for 2 h with a heating rate of 1 °C min^{-1}. The NiO/ZnO core-shell NR arrays were thus obtained after annealing. The bare NiO was obtained by the same cathodic electrdeposition in the solution of 0.01 M $NiCl_2$ + 0.02 M NH_4NO_3 and the subsequent annealing process.

Characterizations

The surface morphology of the samples was observed through scanning electron microscope (SEM, LEO 1530). The structure of the samples was investigated by using transmission electron microscopy (TEM, JEM2010-HR). For the TEM measurement, the prepared samples were mechanically scratched and ground into powders. The scratched specimens were mixed with ethanol, and then were collected with a carbon-coated copper grid. The X-ray powder diffraction (XRD) patterns of the samples were recorded on a diffractometer equipped with Cu Kα (λ = 1.541 Å) radiation (Bruker D8 ADVANCE). X-ray photoelectron spectroscopy (XPS) characterizations were carried on an ESCA Lab 250 (Thermo VG), using a 200 W Al Ka radiation and the analysis chamber pressure was ~7.5 × 10^{-6} Pa. The distance between the sample and X-ray gun was ~1 cm and the pass energy constant was 20 eV for the high resolution scans. The spectra were energy referenced to the C 1s peak of adventitious carbon at 284.8 eV. The diffuse reflectance spectra (DRS) was performed on a Varian Cary 5000 spectrophotometer.

PEC Experiments

PEC experiments were carried out on CHI 660d electrochemical workstation (CHI Instruments) in a typical three-electrode PEC cell with a quartz window to facilitate illumination of the photoelectrode surface. A Pt foil was used as the counter electrode, and an Ag/AgCl electrode was used as the reference electrodes. The prepared NiO/ZnO NR arrays on the FTO substrate acted as the working electrode. The bare ZnO NR arrays were annealed under the same condition and also served as photoanode for comparison measurements. The electrolyte was a 0.5 M Na_2SO_4 aqueous solution (pH = 6.62). A 500 W Xe lamp (PLS-LAX500, Perfectlight) with a water IR filter was used as the illumination source. The illumination intensity at the photoelectrode position was 100 mW cm^{-2}. All PEC experiments were performed at room temperature in air.

Results and discussion

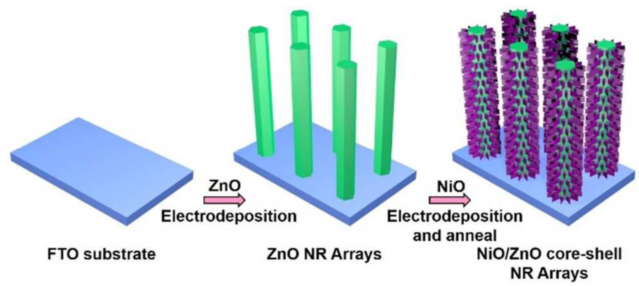

Fig. 1 Schematic procedure for fabricating NiO/ZnO core-shell NR arrays on the FTO substrate.

The NiO/ZnO core-shell NR arrays were obtained by two step electrodepositions and annealing, as schematically shown in Fig. 1. The ZnO NR arrays were first grown on F-doped SnO_2 coated glass (FTO) substrates *via* cathodic electrodeposition. The morphology of the ZnO NR arrays is shown in Fig. 2a. The dense and quasi-aligned ZnO NRs were grown vertically on the substrate. A closer view in Fig. 2b shows that the ZnO NRs have

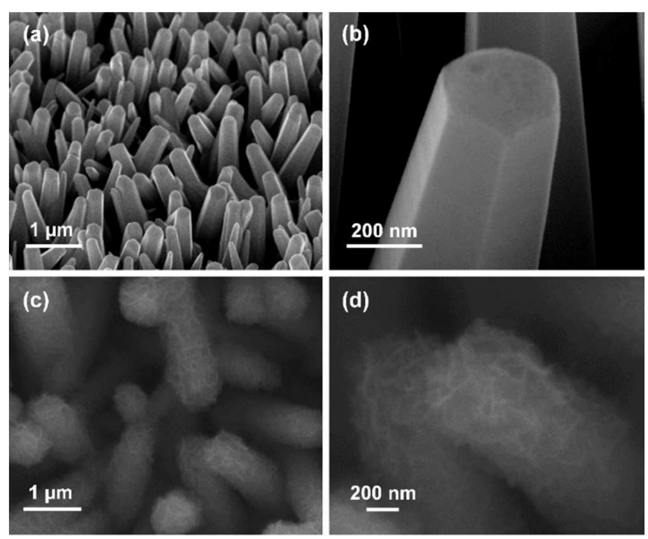

Fig. 2 (a,b) Low- and high-magnification SEM images of ZnO NR arrays, respectively. (c,d) Low- and high-magnification SEM images of as-prepared NiO/ZnO core-shell NR arrays, respectively.

a smooth surface and slightly tempered tips. Subsequently, NiO nanosheets were coatedonto the ZnO NR arrays after the secondary electrodeposition and annealing. The morphology of NiO coating is shown in Fig. 2c, it can be clearly seen that ZnO

NRs were uniformly covered with a rough layer of NiO. As shown in a closer view in Fig. 2d, the ZnO NR was coated by a layer of tiny sheet-like NiO nanostructures. These NiO nanosheets covered the entire ZnO body make the NiO/ZnO core-shell NR possesses a rough and wrinkled surface feature.

Fig. 3a shows the X-ray powder diffraction (XRD) pattern of as-prepared core-shell NRs. All the diffraction peaks can be indexed to hexagonal wurtzite ZnO (JCPDS 36-1451) and FTO substrate. It is worth noting that there is no peak assigned to Ni-based components of the product, which indicates that the Ni-based component of the shell layer is amorphous. In order to further verify the chemical composition of the amorphous coating products, X-ray photoelectron spectroscopy (XPS) characterization were carried out. As shown in Fig. 3b, Zn, O, and Ni signals can be clearly observed in the XPS survey spectrum. KLL and LMM peaks are the Auger spectra related to the electrons of neighboring K, L, and M atomic shells, respectively. Additionally, Si and Cl peaks were also detected, which were originated from the XPS testing substrate and adsorbed electrolyte in electrodeposition process, respectively. Fig. 3c shows the Zn 2p spectrum, and the Zn $2p_{3/2}$ peak centered at 1021.9 eV corresponds to Zn^{2+} in ZnO,[35] which is consistent with the XRD result. The Ni 2p spectrum is illustrated in Fig. 3d. Two Ni satellite peaks are located at the higher binding energy sides of the double Ni 2p peaks. The entire peak shape and the Ni $2p_{3/2}$ peak value (853.9 eV) indicated it is the signature peak of Ni^{2+} in NiO.[36] The transmission electron microscopy (TEM) results revealed that the core-shell NR consists of single crystalline ZnO core and amorphous NiO shell (Fig. S1), which is consistent with the XRD and XPS results. The amorphous NiO nanosheet electrocatalyst shell on single crystalline ZnO NR semiconductor core form a promising composite photoanode configuration that may lead to a significant improvement of the PEC performance.

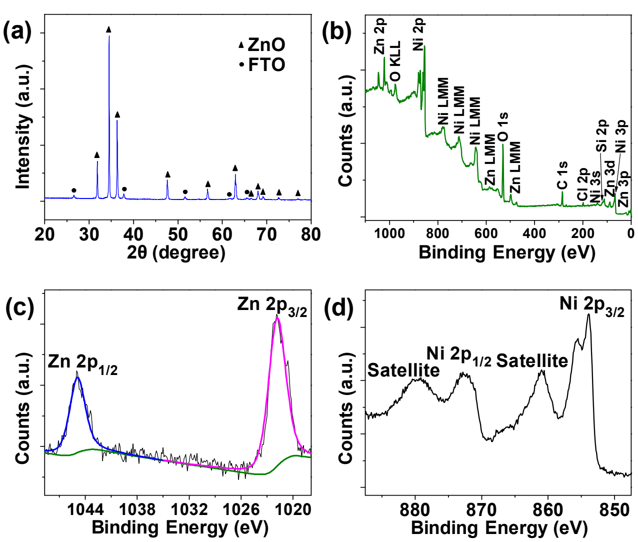

Fig. 3 (a) XRD pattern of the NiO/ZnO core-shell NR arrays. XPS spectrum of (b) survey scan, (c) Zn 2p, and (d) Ni 2p for the NiO/ZnO core-shell NR arrays.

The current-voltage (*J-V*) curves were measured to characterize the PEC performance of the NiO/ZnO core-shell NR and bare ZnO NR photoanodes. The solar-to-hydrogen conversion efficiencies (η) were calculated from these *J-V* curves under illumination. The detailed calculation process and PEC performance parameters (Table S1) are shown in Supporting Information. In the dark scans, the NiO/ZnO photoanode exhibited obvious higher dark current density from 0.65 to 1.6 V compared to the bare ZnO photoanode (inset of Fig. 4a). Because ZnO NR arrays only act as a conductive substrate in the NiO/ZnO photoelectrode in dark scan, the high dark current density of the NiO/ZnO photoanode evidenced the electrocatalytic activity of NiO electrocatalysts. Upon illumination, the NiO/ZnO photoanode exhibited an obvious PEC photocurrent enhancement relative to the bare ZnO photoanode (Fig. 4a). The enhancement of photocurrent was also obtained below the thermodynamic potential for O_2 evolution $E^{\Theta}_{H_2O/O_2}$, which is 1.23 V vs. the reversible hydrogen electrode (RHE). The photocurrent value at 1.23 V vs. RHE is 1.87 mA cm^{-2} for the NiO/ZnO photoanode and 0.04 mA cm^{-2} for the ZnO photoanode (inset of Fig. 4a), respectively. The NiO/ZnO photoanode also yielded a 260 mV cathodic shift in the onset potential for water oxidation compared to the ZnO photoanode. The remarkable cathodic shift evidences the effective electrocatalytic activity of NiO catalyst in oxygen evolution reaction.[37] This cathodic shift of onset potential

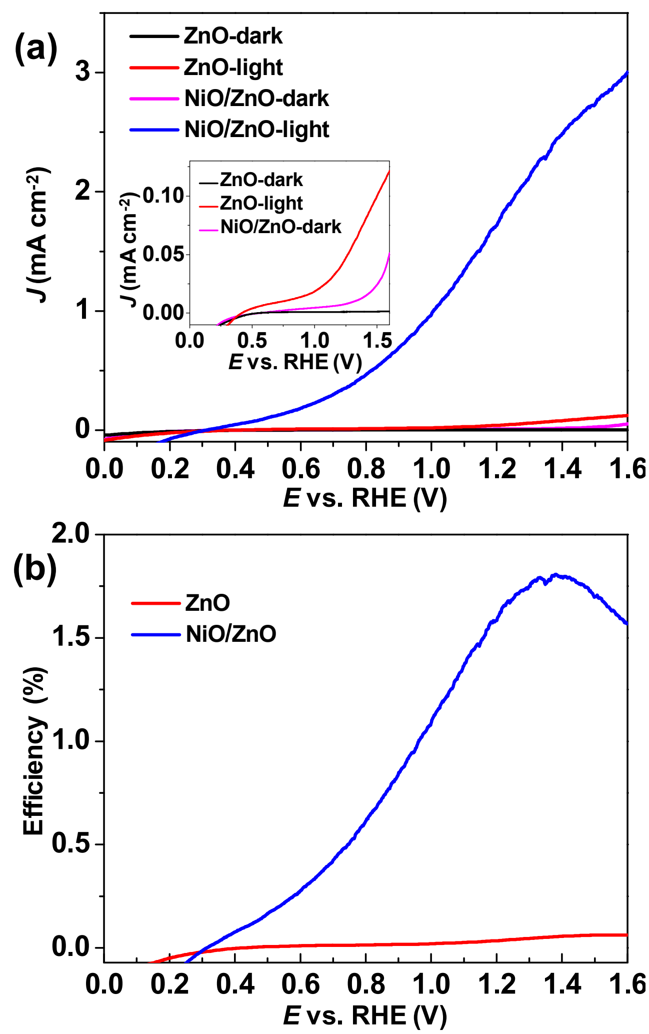

Fig. 4 (a) *J-V* curves of bare ZnO NR and NiO/ZnO core-shell NR photoanodes. Inset shows the magnified dark scans of ZnO and NiO/ZnO photoanodes, and the magnified photocurrent of the ZnO photoanode. (b) The calculated conversion efficiencies as a function of the applied bias for ZnO and NiO/ZnO photoanodes.

is also a competitive value compared to Ga_2O_3/α-Fe_2O_3 photoanode (>100 mV),[38] Co-Pi/$BiV_{0.98}Mo_{0.02}O_4$ photoanode (~150 mV),[13] Co-Pi/WO_3 photoanode (170 mV),[12] $CoCp_2/O_3$/α-Fe_2O_3 photoanode (200 mV),[39] Co-Pi/ZnO photoanode (230 mV),[10] and Co-Pi/α-Fe_2O_3 photoanode (~100 - 230 mV).[11, 40, 41] The photocurrent stability measurements of the NiO/ZnO and ZnO photoanodes were also performed as shown in Fig. S2. The NiO/ZnO photoanode exhibited an improved stability compared to the bare ZnO photoanode. As to the PEC efficiency (shown in Fig. 4b), the NiO/ZnO photoanode achieved the highest efficiency of 1.81%, and it is 30 times enhancement compared to the bare ZnO photoanode (0.06%). This efficiency value is higher than the recentreported values of other ZnO based photoanodes, e.g. undoped ZnO NRs (0.02% - 0.08%),[42, 43] C-doped ZnO (0.18%),[44] $Zn_{0.96}Cu_{0.04}O$ (0.21%),[45] N-doped ZnO (0.1% - 0.31%),[9, 42, 43] Si/ZnO heterostructure (0.38%),[46] $Ni(OH)_2$/ZnO (0.43%),[19] carbon nanotubes modified ZnO (0.65%),[47] CuO/ZnO heterostructure (0.71%),[48] and Ag decorated ZnO (0.81%).[49] These PEC measurement results demonstrates that the NiO electrocatalysts can largely improve the PEC performance of conventional ZnO photoanode.

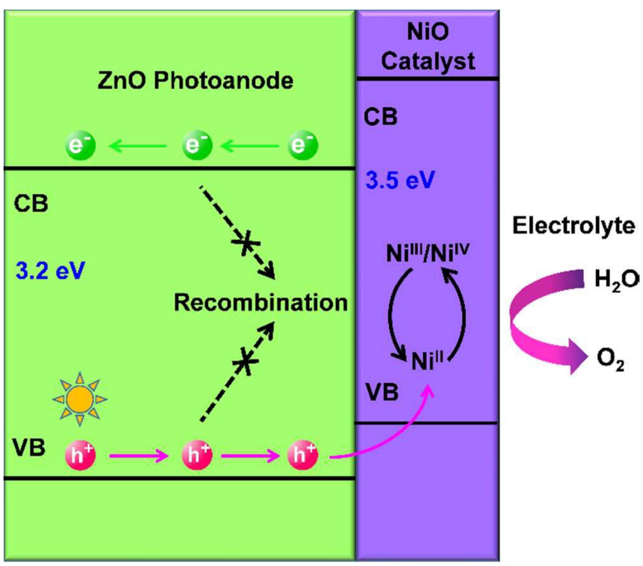

Fig. 5 The band alignment and schematic PEC kinetic processes of NiO/ZnO photoanode.

The band alignment and enhancement mechanism of the NiO/ZnO photoanode is schematically shown in Fig. 5. The diffuse reflectance spectra (DRS) of bare ZnO, NiO/ZnO, and bare NiO were shown in Fig. S3a. The band gap (E_g) values of NiO and ZnO were determined to be 3.5 and 3.2 eV, respectively (Fig. S3b). Upon light irradiation, the initial electron-hole pairs can be generated in ZnO semiconductor by absorbing photons with energy higher than its band gap. In the case of n-type photoanode, photogenerated electrons in the conduction band (CB) of ZnO move toward the counter electrode for the reduction of water. The excited holes in the valance band (VB) of ZnO transfer to the outer NiO catalyst layer. The holes are then captured by NiO and oxidize its Ni^{II} to higher valence Ni^{III}/Ni^{IV}. The higher valence Ni^{III}/Ni^{IV} drives water oxidation reaction, which will be reduced back to Ni^{II}.[50, 51] Introducing the $Ni^{II}/Ni^{III}/Ni^{IV}$ redox processes can effectively reduce the energy barrier of water oxidation reaction, which evidenced by the cathodic shift of onset potential in Fig. 4a. Additionally, the amorphous NiO can provide a large density of active unsaturated sites on the surface to facilitate the holes trapping, and then the direct surface recombination of electron–hole pairs is suppressed. Thus, the PEC performance of conventional ZnO photoanode is significantly improved by introducing NiO electrocatalysts onto its surface.

Conclusions

In summary, we successfully demonstrated an amorphous NiO/single crystalline ZnO core-shell NR arrays photoanode for PEC water splitting. The single crystalline ZnO NR core served as photon absorber and rapid charge transporter, whilst the amorphous NiO shell acted as electrocatalyst to promote the surface oxygen evolution reaction. A remarkable 260 mV cathodic shift in the onset potential for water oxidation was obtained from the NiO/ZnO photoanode compared to the bare ZnO photoanode. The PEC efficiency of the NiO/ZnO photoanode was found to be 1.81%, which is 30 folds enhancement than that was produced by the ZnO photoanode (0.06%). This efficiency value is also much higher than that of $Ni(OH)_2$/ZnO photoanode (0.43%).[19] This work demonstrated introducing amorphous NiO electrocatalysts can effectively improve the PEC performance of conventional ZnO photoanodes. It provides a promising solution to develop high-performance PEC photoanode.

Acknowledgements

E.L. thanks the financial support of the NSFC (No.11104252) and the Education Commission of China (No.20114101110003) and the fund for Science & Technology innovation team of Zhengzhou (No.112PCXTD337). Y.T. thanks the financial support of the NSFC (No.21476271)

Notes and references

[a] *MOE Laboratory of Materials Physics, School of Physical Science and Engineering, Zhengzhou University, Zhengzhou 450052, China, Email: ejliang@zzu.edu.cn*
[b] *School of Chemistry and Chemical Engineering, Sun Yat-sen University, Guangzhou 510275, China*
[c] *Instrumental Analysis and Research Centre, Sun Yat-sen University, Guangzhou 510275, China*

† Electronic Supplementary Information (ESI) available: [Method section, TEM results, photocurrent stability performance, calculation process of the PEC conversion efficiency, DRS spectra, and the summary of performance parameters]. See DOI: 10.1039/b000000x/

1. T. W. Kim and K. S. Choi, *Science*, 2014, **343**, 990-994.
2. F. Le Formal, E. Pastor, S. D. Tilley, C. A. Mesa, S. R. Pendlebury, M. Grätzel and J. R. Durrant, *J. Am. Chem. Soc.*, 2015, **137**, 6629-6637.
3. P. Gao, H. Ma, J. Yang, D. Wu, Y. Zhang, B. Du, D. Fan and Q. Wei, *New J. Chem.*, 2015, **39**, 1483-1487.

4. Y. Su, K. Xiao, Z. Liao, Y. Zhong, N. Li, Y. Chen and Z. Liu, *Int. J. Hydrogen Energy* 2013, **38**, 15019-15026.
5. S. D. Tilley, M. Cornuz, K. Sivula and M. Grätzel, *Angew. Chem. Int. Ed.*, 2010, **49**, 6405-6408.
6. M. P. Dare-Edwards, J. B. Goodenough, A. Hamnett and P. R. Trevellick, *J. Chem. Soc. Faraday Trans.*, 1983, **79**, 2027-2041.
7. M. Gratzel, *Nature*, 2001, **414**, 338-344.
8. J. Shi, M. B. Starr, H. Xiang, Y. Hara, M. A. Anderson, J. Seo, Z. Ma and X. Wang, *Nano Lett.*, 2011, **11**, 5587-5593.
9. X. Y. Yang, A. Wolcott, G. M. Wang, A. Sobo, R. C. Fitzmorris, F. Qian, J. Z. Zhang and Y. Li, *Nano Lett.*, 2009, **9**, 2331-2336.
10. E. M. P. Steinmiller and K. S. Choi, *Proc. Natl. Acad. Sci. U. S. A.,* 2009, **106**, 20633-20636.
11. M. Barroso, A. J. Cowan, S. R. Pendlebury, M. Gratzel, D. R. Klug and J. R. Durrant, *J. Am. Chem. Soc.*, 2011, **133**, 14868-14871.
12. J. A. Seabold and K. S. Choi, *Chem. Mater.*, 2011, **23**, 1105-1112.
13. S. K. Pilli, T. E. Furtak, L. D. Brown, T. G. Deutsch, J. A. Turner and A. M. Herring, *Energy Environ. Sci.*, 2011, **4**, 5028-5034.
14. M. Dinca, Y. Surendranath and D. G. Nocera, *Proc. Natl. Acad. Sci. U. S. A.*, 2010, **107**, 10337-10341.
15. X. Wang, H. Luo, H. Yang, P. J. Sebastian and S. A. Gamboa, *Int. J. Hydrogen Energy* 2004, **29**, 967-972.
16. B. S. Yeo and A. T. Bell, *The J. Phys. Chem. C*, 2012, **116**, 8394-8400.
17. Y. Z. Su, Q. Z. Xu, G. F. Chen, H. Cheng, N. Li and Z. Q. Liu, *Electrochim. Acta* 2015, **174**, 1216-1224.
18. H. Cheng, Y. Z. Su, P. Y. Kuang, G. F. Chen and Z. Q. Liu, *J. Mater. Chem. A*, 2015.
19. Y. Mao, H. Yang, J. Chen, J. Chen, Y. Tong and X. Wang, *Nano Energy*, 2014, **6**, 10-18.
20. K. Sun, N. Park, Z. L. Sun, J. G. Zhou, J. Wang, X. L. Pang, S. H. Shen, S. Y. Noh, Y. Jing, S. H. Jin, P. K. L. Yu and D. L. Wang, *Energy Environ. Sci.*, 2012, **5**, 7872-7877.
21. R. D. L. Smith, M. S. Prevot, R. D. Fagan, Z. P. Zhang, P. A. Sedach, M. K. J. Siu, S. Trudel and C. P. Berlinguette, *Science*, 2013, **340**, 60-63.
22. E. Tsuji, A. Imanishi, K. Fukui and Y. Nakato, *Electrochim. Acta,* 2011, **56**, 2009-2016.
23. Y. Bu, Z. Chen and W. Li, *Dalton Trans.*, 2013, **42**, 16272-16275.
24. D. D. Qin and C. L. Tao, *RSC Advances*, 2014, **4**, 16968-16972.
25. H. M. Chen, C. K. Chen, Y. C. Chang, C. W. Tsai, R. S. Liu, S. F. Hu, W. S. Chang and K. H. Chen, *Angew. Chem. Int. Ed.*, 2010, **49**, 5966-5969.
26. Z. Q. Liu, X. H. Xie, Q. Z. Xu, S. H. Guo, N. Li, Y. B. Chen and Y. Z. Su, *Electrochim. Acta* 2013, **98**, 268-273.
27. J. Miao, H. B. Yang, S. Y. Khoo and B. Liu, *Nanoscale*, 2013, **5**, 11118-11124.
28. P. Y. Kuang, Y. Z. Su, K. Xiao, Z. Q. Liu, N. Li, H. J. Wang and J. Zhang, *ACS Appl. Mater. Interfaces* 2015, **7**, 16387-16394.
29. Y. K. Hsu, S. Y. Fu, M. H. Chen, Y. C. Chen and Y. G. Lin, *Electrochim. Acta* 2014, **120**, 1-5.
30. P. Y. Kuang, Y. Z. Su, G. F. Chen, Z. Luo, S. Y. Xing, N. Li and Z. Q. Liu, *Appl. Surf. Sci.,* 2015, DOI: 10.1016/j.apsusc.2015.08.066.
31. J. Xiao, X. Zhang and Y. Li, *Int. J. Hydrogen Energy* 2015, **40**, 9080-9087.
32. J. Jiang, X. Zhang, P. Sun and L. Zhang, *J. Phys. Chem. C*, 2011, **115**, 20555-20564.
33. P. Kuang, J. Ran, Z. Liu, H. Wang, N. Li, Y. Su, Y. Jin and S. Qiao, *Chem. Eur. J.*, 2015, **21**, 1-10.
34. M. Shao, F. Ning, M. Wei, D. G. Evans and X. Duan, *Adv. Funct. Mater.*, 2014, **24**, 580-586.
35. L. L. Sun, G. Wei, Y. H. Song, Z. G. Liu, L. Wang and Z. Li, *Mater. Lett.*, 2006, **60**, 1291-1295.
36. N. S. McIntyre, T. C. Chan and C. Chen, *Oxid. Met.*, 1990, **33**, 457-479.
37. D. K. Zhong, J. Sun, H. Inumaru and D. R. Gamelin, *J. Am. Chem. Soc.*, 2009, **131**, 6086-6087.
38. M. Barroso, C. A. Mesa, S. R. Pendlebury, A. J. Cowan, T. Hisatomi, K. Sivula, M. Gratzel, D. R. Klug and J. R. Durrant, *Proc. Natl. Acad. Sci. U. S. A.,* 2012, **109**, 15640-15645.
39. S. C. Riha, B. M. Klahr, E. C. Tyo, S. Seifert, S. Vajda, M. J. Pellin, T. W. Hamann and A. B. F. Martinson, *ACS Nano*, 2013, **7**, 2396-2405.
40. D. K. Zhong, M. Cornuz, K. Sivula, M. Graetzel and D. R. Gamelin, *Energy Environ. Sci.*, 2011, **4**, 1759-1764.
41. B. Klahr, S. Gimenez, F. Fabregat-Santiago, J. Bisquert and T. W. Hamann, *J. Am. Chem. Soc.*, 2012, **134**, 16693-16700.
42. Y. C. Qiu, K. Y. Yan, H. Deng and S. H. Yang, *Nano Lett.*, 2012, **12**, 407-413.
43. O. Game, U. Singh, A. A. Gupta, A. Suryawanshi, A. Banpurkar and S. Ogale, *J. Mater. Chem.*, 2012, **22**, 17302-17310.
44. S. T. Kochuveedu, Y. H. Jang, Y. J. Jang and D. H. Kim, *J. Mater. Chem. A*, 2013, **1**, 898-905.
45. Y. K. Hsu and C. M. Lin, *Electrochim. Acta* 2012, **74**, 73-77.
46. M. Shi, X. Pan, W. Qiu, D. Zheng, M. Xu and H. Chen, *Int. J. Hydrogen Energy* 2011, **36**, 15153-15159.
47. Y. Wei, H. Du, J. Kong, X. Lu, L. Ke and X. W. Sun, *Electrochim. Acta* 2014, **143**, 188-195.
48. X. Zhao, P. Wang and B. Li, *Chem Commun*, 2010, **46**, 6768-6770.
49. Y. F. Wei, L. Ke, J. H. Kong, H. Liu, Z. H. Jiao, X. H. Lu, H. J. Du and X. W. Sun, *Nanotechnology*, 2012, **23**.
50. Pourbaix, Marcel and N. d. Zoubov., *Atlas d'équilibres électrochimiques*, Paris: Gauthier-Villars, 1963.
51. K. Juodkazis, J. Juodkazyte, R. Vilkauskaite and V. Jasulaitiene, *J. Solid State Electrochem.*, 2008, **12**,

1469-1479.

Amorphous NiO Electrocatalyst Overcoated ZnO Nanorod Photoanode for Enhanced Photoelectrochemical Performance

Yanchao Mao,[a] Yongguang Cheng,[a] Junqiao Wang,[a] Hao Yang,[b] Mingyang Li,[b] Jian Chen,[c] Mingju Chao,[a] Yexiang Tong,[b] Erjun Liang[a*]

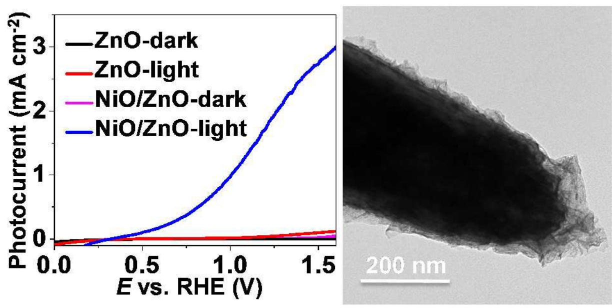

This research demonstrated that introducing amorphous NiO electrocatalysts to the surface of ZnO photoanodes can effectively facilitate their PEC performance.